Published in final edited form as:

Proc IEEE Int Symp Biomed Imaging. 2017 ; 2017: 105–108. doi:10.1109/ISBI.2017.7950479.

A NETWORK APPROACH TO EXAMINING INJURY SEVERITY IN PEDIATRIC TBI

Emily L. Dennis[1,2], **Faisal Rashid**[1], **Neda Jahanshad**[1], **Talin Babikian**[2,6], **Richard Mink**[3], **Christopher Babbitt**[4], **Jeffrey Johnson**[5], **Christopher C. Giza**[6], **Robert F. Asarnow**[2,7], and **Paul M. Thompson**[1,2,8]

[1]Imaging Genetics Center, Keck School of Medicine of USC, Marina del Rey, CA, USA

[2]Department of Psychiatry and Biobehavioral Sciences, Semel Institute for Neuroscience and Human Behavior, UCLA, Los Angeles, CA, USA

[3]Harbor-UCLA Medical Center and Los Angeles BioMedical Research Institute, Department of Pediatrics, Torrance, CA, USA

[4]Miller Children's Hospital, Long Beach, CA, USA

[5]LAC+USC Medical Center, Department of Pediatrics, Los Angeles, CA, USA

[6]UCLA Brain Injury Research Center, Dept. of Neurosurgery and Division of Pediatric Neurology, Mattel Children's Hospital, Los Angeles, CA, USA

[7]Department of Psychology, UCLA, Los Angeles, CA, USA

[8]Departments of Neurology, Pediatrics, Psychiatry, Radiology, Engineering, and Ophthalmology, USC, Los Angeles, CA

Abstract

Traumatic brain injury (TBI) is the leading cause of death and disability in children, and can lead to long lasting functional impairment. Many factors influence outcome, but imaging studies examining effects of individual variables are limited by sample size. Roughly 20–40% of hospitalized TBI patients experience seizures, but not all of these patients go on to develop a recurrent seizure disorder. Here we examined differences in structural network connectivity in pediatric patients who had sustained a moderate-severe TBI (msTBI). We compared those who experienced early post-traumatic seizures to those who did not; we found network differences months after seizure activity stopped. We also examined correlations between network measures and a common measure of injury severity, the Glasgow Coma Scale (GCS). The global GCS score did not have a detectable relationship to brain integrity, but sub-scores of the GCS (eyes, motor, verbal) were more closely related to imaging measures.

Index Terms

traumatic brain injury; early post-traumatic seizure; graph theory; diffusion MRI

1. INTRODUCTION

Traumatic brain injury (TBI) can cause long-lasting damage to the brain, especially in children whose brains are still developing. Some patients recover fully, while others experience prolonged deficits. Severity of the acute injury accounts for some of this variability, but many other factors are thought to contribute to this variation. Here we examined one of these injury variables – early post-traumatic seizures.

Some patients suffer from post-traumatic epilepsy (PTE) after an injury, but a subset of patients who suffer seizures immediately post-injury do not go on to develop a recurrent seizure disorder. Seizures that only occur within a week of the injury are classified as early post-traumatic seizure, and occur in 4–25% of patients (1, 2). Most of the existing literature regarding imaging and post-traumatic seizures seeks to improve prediction - immediately post-injury - of which patients will develop EPTS, or which patients with EPTS will later develop PTE. Risk factors for EPTS include injury severity, younger age (in children), and cortical damage (3, 4) and it is associated with poorer outcomes (5).

The Glasgow Coma Scale (GCS) is the most commonly used measure of injury severity in TBI. Some recent papers regard it as a relatively blunt tool in understanding the pathophysiology of TBI (6). Recent imaging studies from our group failed to find significant relationships between GCS and imaging biomarkers (7–9). GCS is a 3–15 scale comprised of separate scores for eye, verbal, and motor function, with 3 being deep unconsciousness (10). We examined associations between structural network measures and GCS as well as its component scores to determine what use this measure may have as a biomarker of brain integrity.

2. METHODS

2.1 Subjects and Image Acquisition

TBI participants were recruited from 4 Pediatric Intensive Care Units (PICUs) at Level 1 and 2 Trauma Centers in Los Angeles County. Participants were studied in the post-acute phase (2–5 months post-injury) and assessed again 12 months later. We included 34 TBI participants (25 M/9 F, average age 14.2). *Inclusion criteria*: non penetrating moderate-severe TBI (intake or post-resuscitation GCS score between 3 and 12, or with higher GCS but positive imaging findings), 8–18 years old, right handed, normal vision, English proficiency. *Exclusion criteria*: history of neurological illness or injury (including post-traumatic epilepsy), motor deficits or a metal implant preventing safe MRI scanning, history of psychosis, ADHD, Tourette's, learning disability, mental retardation, autism, or substance abuse.

Participants were scanned using 3T MRI (Siemens Trio) with whole-brain anatomical and 72-gradient diffusion imaging. Diffusion-weighted images (DWI) were acquired with the following parameters: GRAPPA mode; acceleration factor PE=2; TR/TE=9500/87 ms; FOV=256×256mm; isotropic voxel size=2 mm. 72 images were collected per subject: 8 b_0 and 64 diffusion-weighted images (b=1000 s/mm^2).

During the study, scanning moved to a different scanner at UCLA – yet the make, model and scan parameters remained consistent. Extensive testing was conducted with volunteer and phantom data to ensure no bias was introduced with respect to the study design. Details may be found in (7).

2.2 Cortical Extraction and Tractography

Connectivity analysis was performed as in (11). Briefly, non-brain regions were automatically removed from each T1-weighted MRI scan, and from the dMRI scan, using the FSL tool "BET" (FMRIB Software Library, http://fsl.fmrib.ox.ac.uk/fsl/). A neuroanatomical expert manually edited the T1-weighted scans to refine the brain extraction. All T1-weighted images were linearly aligned using FSL (with 9 DOF) to a common space with $1mm$ isotropic voxels and a 220×220×220 voxel matrix. For each subject, the 8 eddy-corrected images (using FSL tool "eddy_correct" http://fsl.fmrib.ox.ac.uk/fsl/) with no diffusion sensitization were averaged, linearly aligned and resampled to a downsampled version of their corresponding T1 image (110×110×110, 2×2×2mm). Averaged b_0 maps were elastically registered to the structural scan using a mutual information cost function to compensate for EPI-induced susceptibility artifacts. 34 cortical labels per hemisphere, as listed in the Desikan-Killiany atlas (12), were automatically extracted from all aligned T1-weighted structural MRI scans using FreeSurfer (http://surfer.nmr.mgh.harvard.edu/). T1-weighted images and cortical models were aligned to the original T1 input image space and down-sampled to the space of the DWIs, using nearest neighbor interpolation (to avoid intermixing of labels). To ensure tracts would intersect cortical labeled boundaries, labels were dilated with an isotropic box kernel of size 5×5×5 voxels.

The matrix transforming the mean b_0 image to the T1-weighted volume was applied to each of the 64 gradient directions to properly re-orient the orientation distribution functions (ODFs). At each dMRI voxel, ODFs were computed using the normalized and dimensionless ODF estimator, derived for q-ball imaging (QBI). We performed HARDI tractography on the linearly aligned sets of DWI volumes using these ODFs, using the Hough transform method (13). Elastic deformations obtained from the EPI distortion correction, mapping the average b_0 image to the T1-weighted image, were then applied to the tracts' 3D coordinates to accurately align the anatomy. Each subject's dataset contained 35,000–50,000 useable fibers (3D curves). For each subject, a full 68×68 connectivity matrix was created. Each element described the proportion of the total number of detected fibers connecting each of the labels; diagonal elements describe the total number of fibers passing through a certain cortical region of interest. Values were calculated as a proportion - normalized by the total number of fibers traced for each individual participant and by the volume of the two terminal ROIs. This was done so that results were not skewed by raw fiber count or by a tracking bias favoring large ROIs.

2.3 Graph Theory Analyses

On the count- and volume-normalized 68×68 fiber density matrices, we used the Brain Connectivity Toolbox ((14); https://sites.google.com/site/bctnet/) to compute the following network metrics: CPL (characteristic path length – average path length in network), MCC (mean clustering coefficient – degree of clustering in network), EGLOB (global efficiency –

approximately inverse of CPL), SW (small-worldness – ratio of local clustering to path length), and MOD (modularity – degree to which network can be subdivided into modules). We generated 50 simulated random networks, with the same degree distribution and number of nodes. The ratio of clustering coefficient in our network to the mean value obtained for a simulated random network was denoted by *lambda* (λ). The ratio of CPL in our network to the mean CPL in simulated random networks was denoted by *gamma* (γ). All measures were calculated for the network as a whole, based on (14).

For *post hoc* analyses, we also calculated nodal topology measures, including degree (DG), clustering coefficient (CC) and regional efficiency (EREG).

2.4 Statistics

All statistics were run within the TBI patient group only, comparing those who suffered from EPTS to those who did not. We examined group differences in global BCT metrics. To run these analyses, we ran regressions using these models:

$$Y \sim A+\beta_{age}Age+\beta_{sex}Sex+\beta_{scanner}Scanner+\beta_{EPTS}EPTS+$$

Here Y is any of the BCT network measures, A is a constant for each regression model, the βs are the covariate regression coefficients, and ε is an error term. We also ran a model including GCS (Glasgow Coma Scale) as a covariate. All tests were corrected for multiple comparisons (15).

3. RESULTS

3.1 EPTS

Of the 34 TBI patients in the post-acute phase, 10 suffered from EPTS and 24 did not, which is consistent with reported rates (16). Not all of these patients continued the study. Of the 25 patients who participated in the follow-up, 9 suffered from EPTS and 16 did not. Comparing TBI patients who suffered EPTS to those who did not in the chronic phase, we found significant differences in MCC (p=0.012) and MOD (p=0.014). TBI patients with EPTS had greater MCC and lower MOD. These associations were borderline in the post-acute phase (p=0.044 and p=0.0098, respectively). These were FDR corrected across all 7 measures tested, separately within each time-point.

When covarying for GCS, the significant differences in chronic MCC remained (p=0.0091), but the differences in MOD were only borderline (p=0.024). TBI patients with EPTS now also registered lower γ (p=0.011). The post-acute differences in MCC remained borderline (p=0.0078).

3.2 GCS

As GCS affected our results above, we also examined whether GCS was associated with global graph theory metrics, across all TBI patients, after adjusting for covariates. We found a nominal association between GCS and post-acute MOD (p=0.020), but no associations in the chronic phase.

We also separated GCS into its component scores – eyes, motor, and verbal, and examined associations with these scores. We found a significant association between GCS-eyes and post-acute MOD (p=0.0019), when correcting across all 7 global measures. Patients with a higher GCS-eyes score had higher MOD. Neither GCS-motor nor GCS-verbal registered any associations with global graph theory metrics. None of the sub-scores was associated with chronic global metrics at p<0.05.

We also examined nodal measures *post hoc* with each of these sub-scores. GCS-eyes had no significant associations with nodal measures. In the chronic phase, GCS-motor showed borderline associations with degree in the right lateral orbitofrontal gyrus (p=0.0012) and right rostral anterior cingulate (p=0.00044). Patients with higher GCS-motor had lower degree in these nodes. These were significant correcting across all nodes tested (68), but not across all measures (3). In the post-acute phase, GCS-verbal showed borderline associations with clustering coefficient in the left peri-calcarine node (p=0.00041). In the chronic phase, GCS-verbal showed borderline associations with clustering coefficient in the left *pars opercularis* (p=0.00091), and clustering coefficient and regional efficiency of the right banks of the superior temporal sulcus (p=0.0015). Patients with higher GCS-verbal had lower clustering and higher regional efficiency for these nodes.

Lastly, we examined the underlying 68×68 fiber density matrices. Here we found associations between GCS-motor and the fiber density of the connections between the left lateral orbitofrontal gyrus and the left rostral anterior cingulate (p= 0.00033), the left lateral orbitofrontal gyrus and the right rostral anterior cingulate (p=0.00046), and between the right lateral orbitofrontal gyrus and the right rostral anterior cingulate (p=0.00013). For all of these, patients with a lower GCS-motor had a higher fiber density. These results are shown in Figure 1.

4. DISCUSSION

We examined injury variables in pediatric TBI, specifically early post-traumatic seizure activity, and components of the Glasgow Coma Scale (GCS). We found greater network clustering and shorter normalized path length in patients who had suffered from early post-traumatic seizures (EPTS) 13–19 months prior. This may suggest a more efficient network, but global efficiency was not significantly different. With small groups (16 vs. 9), outliers can significantly impact results as well. Risk factors for EPTS in children include injury severity and age (3, 4) but neither of these variables were significantly different between the groups (p=0.16 and p=0.74 respectively), and both were included as covariates in the regression. EPTS is associated with worse outcome, including severe disability and death, but we found further long-term alterations even among patients healthy enough to complete our study protocol.

The association between GCS and post-acute MOD appears to be driven by the GCS-eyes component, as neither GCS-verbal nor GCS-motor registered any association with this measure. Modularity is a measure of network separation. Patients with high GCS-eyes score had higher MOD post-acutely, perhaps indicating that having a network characterized by well-established modules supports this distributed function. The GCS-eyes scale depends

upon a set of intact functions – opening eyes in response to pain, in response to verbal commands, or spontaneously. These are not purely eye functions but also include processing external stimuli, which may explain its dependence on intact global function. For this association, our N was higher (33) and we performed a linear regression, not a group *t*-test, so we have more confidence in these results.

GCS-verbal showed trend-level associations with clustering in two regions associated with verbal processing in the chronic phase – the left *pars opercularis* (also known as Broca's area, key for language processing (17)) and the right banks of the superior temporal sulcus, which plays a role in processing auditory input (18).

GCS-motor showed trend-level associations with degree in the right lateral orbitofrontal gyrus and right rostral anterior cingulate gyrus. These nodes also showed lower fiber density in patients with higher GCS-motor scores. The OFC is densely connected with the motor cortex, and is thus thought to play a role in the executive control of motor function (19). The directions of these results are unexpected, and perhaps point to compensatory processes at play in patients with poorer motor function immediately post-injury.

Our analyses with nodal measures were only significant at a trend-level, passing correction for the number of nodes tested but not for the number of measures. For this reason, we consider these results as preliminary and in need of a bigger sample size. However, they do suggest that the global GCS score has little relation to brain measures, and that researchers and clinicians might be better served by considering the individual scores that make up the GCS. Predicting outcome post-TBI is still difficult, and any information that may improve this prediction for the clinician is beneficial. With better outcome prediction, clinicians can identify patients who might benefit from more aggressive treatment and help families have accurate expectations.

5. CONCLUSION

In this paper, we examined graph theory measures of structural connectivity in pediatric TBI patients, focusing on acute injury variables that may be associated with alterations in network topology months later. We found that patients who had experienced seizures in the first week post-injury (EPTS) show network alterations months post-injury. We also found that the common scale of severity, GCS, has little relation with brain measures, but found more utility in the sub-scores. These are preliminary results that need to be examined in a larger dataset, but could improve outcome prediction.

Acknowledgments

This study was supported by a NICHDS (R01 HD061504) grant to RA. ELD is supported by a grant from the NINDS (K99 NS096116). ELD, FR, NJ, and PT are also supported by NIH grants to PT: U54 EB020403 (BD2K), R01 EB008432, R01 AG040060, and R01 NS080655. CCG is supported by the UCLA BIRC, UCLA Faculty Grants Program, NS027544, Child Neurology Foundation, UCLA Steve Tisch BrainSPORT Program, NCAA, U.S. Dept of Defense and the Today's and Tomorrow's Children Fund. Scanning was supported by the Staglin IMHRO Center for Cognitive Neuroscience. We gratefully acknowledge the contributions of Alma Martinez and Alma Ramirez in assisting with participant recruitment and study coordination. We thank the participants and their families for contributing their time to this study.

References

1. Agrawal A, et al. Post-traumatic epilepsy: an overview. Clin Neurol Neurosurg. 2006; 108:433–439. [PubMed: 16225987]
2. Arndt DH, Goodkin HP, Giza CC. Early Posttraumatic Seizures in the Pediatric Population. Journal of Child Neurology. 2016; 31:46–56. [PubMed: 25564481]
3. Chiaretti A, et al. Early post-traumatic seizures in children with head injury. Child Nerv Syst. 2000; 16:862–866.
4. Annegers JF, et al. A population-based study of seizures after traumatic brain injuries. NEJM. 1998; 338:20–24. [PubMed: 9414327]
5. Ong LC, et al. Early post-traumatic seizures in children: clinical and radiological aspects of injury. J Paediatr Child H. 1996; 32:173–176.
6. Saatman KE, et al. Classification of Traumatic Brain Injury for Targeted Therapies. J Neurotrauma. 2008; 25:719–738. [PubMed: 18627252]
7. Dennis EL, et al. White matter disruption in moderate/severe pediatric traumatic brain injury: advanced tract-based analyses. NeuroImage Clin. 2015; 7:493–505. [PubMed: 25737958]
8. Dennis EL, et al. Callosal function in pediatric traumatic brain injury linked to disrupted white matter integrity. J Neurosci. 2015; 35:10202–10211. [PubMed: 26180196]
9. Dennis EL, et al. Progressive white matter damage in pediatric moderate/severe traumatic brain injury: A longitudinal study. Neurology Accepted. 2016
10. Teasdale G, Jennett B. Assessment of coma and impaired consciousness. A practical scale. Lancet. 1974; 2:81–84. [PubMed: 4136544]
11. Jahanshad N, et al. Sex differences in the human connectome: 4-Tesla high angular resolution diffusion imaging (HARDI) tractography in 234 young adult twins. Proc 8th IEEE ISBI. 2011:939–943.
12. Desikan RS, et al. An automated labeling system for subdividing the human cerebral cortex on MRI scans into gyral based regions of interest. NeuroImage. 2006; 31:968–980. [PubMed: 16530430]
13. Aganj I, et al. A Hough transform global probabilistic approach to multiple-subject diffusion MRI tractography. Med Image Anal. 2011; 15:414–425. [PubMed: 21376655]
14. Bullmore E, Sporns O. Complex brain networks: graph theoretical analysis of structural and functional systems. Nat Rev Neurosci. 2009; 10:186–198. [PubMed: 19190637]
15. Benjamini Y, Hochberg Y. Controlling the false discovery rate: a practical and powerful approach to multiple testing. J Roy Stat Soc B. 1995:289–300.
16. Arndt DH, et al. Subclinical early posttraumatic seizures detected by continuous EEG monitoring in a consecutive pediatric cohort. Epilepsia. 2013; 54:1780–1788. [PubMed: 24032982]
17. Dronkers NF, Plaisant O, Iba-Zizen MT, Cabanis EA. Paul Broca's historic cases: high resolution MR imaging of the brains of Leborgne and Lelong. Brain. 2007; 130:1432–1441. [PubMed: 17405763]
18. Beauchamp MS, et al. Integration of auditory and visual information about objects in superior temporal sulcus. Neuron. 2004; 41:809–823. [PubMed: 15003179]
19. Cavada C, et al. The anatomical connections of the macaque monkey orbitofrontal cortex. A review. Cereb Cortex. 2000; 10:220–242. [PubMed: 10731218]

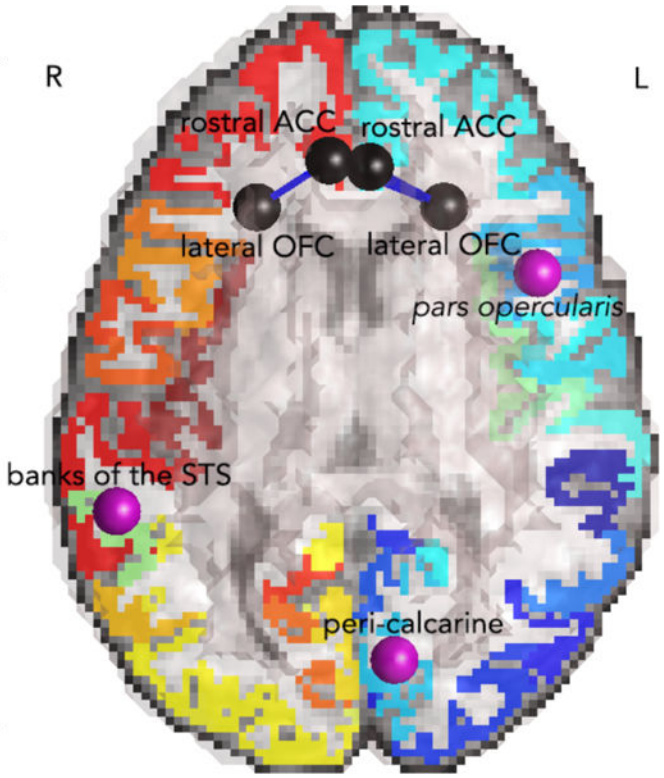

Figure 1.

Nodal results of GCS analyses. Magenta indicates nodes whose measures were assoc. with GCS-verbal, black nodes are those whose measures were assoc. with GCS-motor. Blue connections were assoc. with GCS-motor. STS=superior temporal sulcus, ACC=anterior cingulate cortex, OFC=orbitofrontal cortex. Left in image is right in brain.